CONFIDENTIAL

Copy 1
RM E55D22

NACA RM E55D22

NACA

RESEARCH MEMORANDUM

AN ANALYSIS OF RAM-JET-ENGINE TIME DELAY FOLLOWING A FUEL-FLOW DISTURBANCE

By Fred A. Wilcox and Arthur R. Anderson

Lewis Flight Propulsion Laboratory
Cleveland, Ohio

NATIONAL ADVISORY COMMITTEE FOR AERONAUTICS

WASHINGTON

June 30, 1955

CONFIDENTIAL

NATIONAL ADVISORY COMMITTEE FOR AERONAUTICS

RESEARCH MEMORANDUM

AN ANALYSIS OF RAM-JET-ENGINE TIME DELAY FOLLOWING A FUEL-FLOW DISTURBANCE

By Fred A. Wilcox and Arthur R. Anderson

SUMMARY

After a fuel-flow disturbance in a ram-jet engine, a time delay occurs before the engine responds. After the time delay, there is a rapid change in response followed by a gradual approach to the new steady-state condition. In the analytical method of predicting this initial time delay proposed herein, the delay is assumed to consist of the time for fluid propagation downstream from the fuel injector to the exhaust-nozzle throat plus the time for pressure-wave propagation upstream from the nozzle throat to the sensing station.

In the analysis, the ram-jet engine is studied through individual consideration of its components, namely, the diffuser, fuel-mixing region, combustion chamber and exhaust nozzle. The combustion-chamber time delay was calculated theoretically for several rates of heat addition and compared with experimental values.

An optimum combustor-inlet Mach number is shown to exist for minimum time delay for each condition of combustion-chamber temperature ratio and flight Mach number. Methods of reducing the total engine time delay include (1) using minimum component lengths, especially the fuel-mixing length; (2) using high-reaction-rate fuels; and (3) placing the sensing element as close to the nozzle throat as possible.

INTRODUCTION

The dynamic behavior of the ram-jet engine must be known for the integrated design of the engine and the engine control systems. Much of this required dynamic information can be obtained from the response of the engine to imposed step disturbances. Experimental data (ref. 1) show that, after a step change in fuel flow, the ram-jet engine has a time delay during which no engine response is obtained. References 2 and 3 show how this time delay limits the response rate of engine control systems.

As a step in describing ram-jet-engine dynamics, an analytical means of determining time delay and an insight into the factors affecting this delay are presented and discussed. The total time delay is assumed to consist of the time for fluid propagation downstream from the fuel injector to the nozzle throat plus time for wave propagation upstream from the nozzle throat to the control sensing element. General equations are developed for the fluid- and wave-propagation times through the engine components under a variety of operating conditions. For ease of interpretation and application, these equations have been solved and are presented graphically. The analytically derived results are then compared with the limited experimental data available. This analysis was made at the NACA Lewis laboratory.

ANALYSIS AND COMPUTATIONS

A schematic diagram of the response of internal engine pressure to a step change in fuel flow is presented in figure 1. Following a sudden increase in fuel flow, there is a time delay before the pressure change produced by this new operating condition is sensed at a station s forward of the fuel injector (fig. 2). At the end of this time delay (also termed "dead time"), the sensed pressure rises abruptly at first, and then gradually approaches the new steady-state pressure condition.

In order to understand the proposed mechanism of time delay, consider the schematic diagram of a fixed-geometry ram-jet engine (fig. 2). The time delay is assumed to consist of the propagation time for the fluid particles to travel from the fuel injector to the exit-nozzle throat plus the time for a pressure wave to travel upstream from the throat to the pressure sensing station s in the diffuser. When the temperature change resulting from the fuel-flow disturbance reaches the nozzle throat (the point of choking), a pressure wave traveling upstream at the local speed of sound is produced. Pressure waves due to burning are also transmitted upstream, but these are assumed to be weak. This assumed mechanism is intended to give the minimum possible time delay. No consideration is given to the response of the engine after the time delay. In applying this analysis, it must be noted that the terminal shock must be at or ahead of the sensing station s. For sensing stations ahead of the normal shock, there obviously may be no response.

In analyzing the time delay, it was convenient to treat the engine components separately and then to total the component time delays. The definition of symbols and the derivation of equations for the component time delays are given in appendixes A and B, respectively.

The engine was assumed to be operating in the stratosphere at stream Mach numbers from 2.0 to 4.0. The range of diffuser-exit Mach number investigated varied from 0.10 to 0.25, and the over-all total-temperature ratio τ was varied from 2 to 5.

The following assumptions were made in the analysis:

(1) In the diffuser, the ratio of specific heats γ equals 1.4 and in the combustor and exhaust nozzle $\gamma = 1.3$. The gas constant R was taken as that of air and equal to 1716 $(ft/sec^2)(ft\text{-}lb/(lb)(^oR))$ throughout the engine.

(2) After injection, the fuel is assumed to travel at the local air velocity into the combustor (ref. 4).

(3) The flame front is assumed to move at the initial steady-state air velocity, and combustion is considered to take place in a constant-area combustion chamber. For purposes of estimating the fuel-air ratio, the combustion efficiency is assumed to be 100 percent. Otherwise, combustion efficiency does not enter the analysis, since the results as presented depend only upon the initial and final total temperatures.

(4) The following four alternative curves shown in figure 3 were assumed for the temperature rise in the combustion chamber:

(A) As an extreme condition simulating fuels having extremely high reaction rates, a step-function temperature-rise curve was used. During the transient, no choking was assumed except at the exhaust nozzle.

(B) Since the steady-state temperature-rise variation in a ramjet engine with a conventional hydrocarbon fuel has been shown to approximate the first 90^o of a sine curve (ref. 5), a sine distribution was used. For small-sized fuel steps, this steady-state temperature distribution would closely approximate that occurring during the transient.

(C) For ease of computation and purposes of comparison, a linear temperature variation was assumed.

(D) For large-sized fuel steps, the temperature-rise curve might be expected to droop during the transient (ref. 6). Accordingly, an exponential temperature-length expression which approximates the time-averaged temperature distribution was also evaluated.

(5) Both the exhaust nozzle and the diffuser were assumed to have a linear variation in radius with length and a constant gas total temperature. A range of area ratio A_5/A_4 from 0.5 to 0.8 was used in the nozzle calculations, and the nozzle was assumed to be choked at the throat, station 5.

The fluid- and wave-propagation times, which combine into the total time delay, were computed for the following components: (a) fuel-mixing region, station i to 2; (b) combustion chamber, station 2 to 4; and (c) exhaust nozzle, station 4 to 5. In addition, the wave-propagation time only was computed for a length of diffuser section (station i to s). The results of these calculations per unit length are presented in figures 4 to 11.

The total time delay in the fuel-mixing region is presented in figure 4 as a function of diffuser-exit velocity u_i and diffuser-exit total temperature T_i. For convenience, the accompanying table gives values of u_i and T_i for the range of diffuser-exit Mach number M_i considered. For engines not having a constant fuel-mixing area, the average velocity between stations i and 2 can be used. In order to compare the effect of fluid- and wave-propagation times, the fluid-propagation time was also plotted and is simply $1/u_i$. For most operating conditions, the fluid-propagation time in the fuel-mixing region is considerably greater than the wave-propagation time.

The combustor time delay for the step-function (curve A, fig. 3) heat-addition variation is given in figure 5. The combustor time delay decreases to a minimum with increasing combustor-inlet velocity u_3 and then rises sharply as high stream velocities through the combustion chamber cause large increases in the wave-propagation time. An optimum value of combustor-inlet Mach number M_3 for minimum time delay is indicated on each curve. This minimum time delay decreases with increasing τ and free-stream Mach number M_0. The effect of M_0 is due to changes in combustor-inlet temperature T_3. Similar trends exist in all the other assumed combustor temperature distributions (figs. 6 to 8).

In order to show the relation between fluid- and wave-propagation time, the fluid-propagation time only is plotted on figure 6 also. From these curves it is seen that at the lower inlet velocities the time delay is predominantly fluid-propagation time, but at the higher inlet velocities the time delay is predominantly wave-propagation time. A comparison of the several assumed temperature variations reveals that the more rapid the rate of heat addition, the shorter the time delay. This trend is summarized in table I for the four temperature variations assumed at $\tau = 4$ under identical combustor-inlet conditions.

The curves of figures 5 to 8 are based on combustor-inlet conditions at station 3 and neglect any effect the flameholder may have on the combustor time delay. This effect may be taken into account by correcting the combustor-inlet velocity to include the slight velocity increase due to the pressure drop across the flameholder. From table II it is seen that, at combustor-inlet velocities generally considered for ram-jet application, only a small error in combustor time delay results from neglecting the effect of the flameholder. The error becomes great,

however, near the choking limit for a constant-area nozzle as the inlet velocity becomes large and wave-propagation time becomes dominant, causing the reversal in trend of the relation between velocity and time delay.

The total time delay in a conical exhaust nozzle is given in figure 9 as a function of inlet total temperature T_4 and exit area ratio A_5/A_4. This time delay decreases with an increase in the inlet temperature or a decrease in the contraction ratio.

Since the fuel is injected downstream of the subsonic diffuser, no fluid-propagation time need be considered for the diffuser. The wave-propagation-time parameter of a conical diffuser is presented in figure 10 as a function of area ratio A_i/A_s and inlet and exit Mach numbers. As would be expected, the wave-propagation-time parameter for a conical diffuser of given area ratio is reduced by lowering the velocity through the diffuser.

Inasmuch as some ram-jet diffusers have a combination of constant-area and conical sections, the wave-propagation time per foot through a constant-area section was also computed and is plotted in figure 11 as a function of the flow velocity u and the stream total temperature T.

EXPERIMENTAL AND ANALYTICAL RESULTS AND INDICATED DESIGN TRENDS

Results

Experimental time-delay data were obtained in the Lewis 8- by 6-foot supersonic wind tunnel for a 16-inch ram-jet engine (fig. 12). As reported in reference 1, the experimental time delay for all test conditions varied from 0.02 to 0.05 second. The range in experimental values may be explained on the basis of a variation in (1) the rate of heat addition; (2) the point at which combustion begins; and (3) the location of the terminal (normal) shock before and after the disturbance.

The effect of rate of heat addition on the time delay has already been discussed and is summarized in table I. The effect of a variation in the point at which combustion begins can be seen by assuming combustion to start first at the pilot, station 2' (fig. 12); then at the end of the sleeve, station 2; and finally at the end of the can, station 3. At those stations, with the sine temperature distribution assumed, total engine time delays are 0.0271, 0.0307, and 0.0364 second, respectively. Since the combustor of the 16-inch engine was a can configuration, a change in engine operating condition may easily shift the position along the can where the gas temperature rises.

When step-function, linear, or exponential temperature distributions are assumed, a larger variation results which approximates that obtained

experimentally. Experimental fuel-flow steps were made between slightly supercritical and slightly subcritical engine operation. The measured time delay closely approximated 0.025 second. By assuming the sine temperature distribution and combustion beginning at the pilot (station 2'), good agreement between experimental (0.025 sec) and theoretical (0.027 sec) time delay was obtained.

Data were also taken with the combustion chamber shortened 2 feet. Under the conditions of nearly critical operation, the average experimental time delay was 0.0215 second; with assumptions of the sine temperature distribution and combustion beginning at the pilot, a theoretical time delay of 0.0225 second resulted.

The experimentally observed response of static pressure at station s of this engine to a sinusoidal fuel-flow variation is reported in reference 3 and is reproduced in figure 13. Also included in figure 13 is the theoretically predicted response, considering time delay only. A fair approximation to the experimental response is obtained at the lower frequencies, and good agreement is obtained at the higher frequencies. As stated previously, the response of internal engine pressure to a step change in fuel flow consists of a time delay, an abrupt change in pressure, and then a gradual approach to the new steady-state value. If the initial abrupt change is a sufficiently large part of the total change, satisfactory prediction of the dynamic behavior of certain simple control systems (ref. 2, for example) is possible from time-delay considerations alone. For more complex control systems or where the initial change is not a large part of the total change, knowledge of the gradual approach to the final value is also required.

Unpublished experimental time-delay data are available for a large submerged ram-jet engine, shown schematically in figure 14. With the sensing probes placed at stations 3 and s, total time delays of approximately 0.015 and 0.05 second, respectively, were recorded. Under assumptions of sine-variation rate of heat addition, combustion starting midway between stations i and 3, and by using the measured diffuser-exit Mach number, corresponding time delays of 0.023 and 0.045 second result analytically. When sensed at station s, the time delay was considerably larger than the value obtained at station 3 because of the extreme length of the subsonic diffuser and the high level of Mach number in the section from s to i. Although the combustion-chamber diameter is three times as large as that of the 16-inch engine, similar combustor-time-delay values were obtained as a result of similar component lengths.

Design Trends

Since the total engine time delay obtained analytically is in reasonable agreement with experimental data, component time delays were

examined to determine favorable design trends. Table III lists the component time delays for the 16-inch ram jet assuming the sine temperature variation and operation at a flight Mach number of 2.0 and a diffuser-exit Mach number of 0.185. For this table the engine time delay was evaluated for station s of figure 12. The principal factors contributing to time delay are fuel-injector location and combustion-chamber length. The engine time delay could be reduced up to 22 percent by locating the fuel injector closer to the combustor. As stated previously, the time delay in the combustor could be reduced by shortening the combustion chamber and by selecting the optimum combustor-inlet Mach number indicated in figure 6. However, the combustion efficiency was reduced from 77 to 69 percent at critical operation (ref. 7) by shortening the combustion chamber. Reductions in chamber length may be achieved without losses in combustion efficiency by utilizing a fuel having a higher reaction rate.

Engine wave-propagation time in the diffuser may be reduced by eliminating straight sections, shortening the diffuser, and by keeping the Mach number low downstream of the sensing station. Finally, for control systems other than inlet-shock positioning devices, the engine time delay can be reduced considerably by locating the control sensor as close to the exit-nozzle throat as possible.

CONCLUDING REMARKS

A method has been developed to estimate ram-jet-engine time delay following a fuel-flow disturbance. The method is based upon the assumption of a fluid-propagation time from the fuel injector to the exhaust-nozzle throat plus a wave-propagation time upstream from the nozzle throat to the control sensing station. Over-all time delays predicted by this method show reasonable agreement with experiment. An analysis of engine components suggests that short lengths of all components are desirable for obtaining low values of time delay. For engines that employ a fuel-injection system upstream of the flameholder, a reduction in the fuel-mixing length offers a means for appreciably lowering the time delay. In addition, the time delay can be reduced by using high-reaction-rate fuels and by designing for an optimum combustor-inlet Mach number. The time delay of the engine control loop can also be reduced substantially by employing control systems with the sensing station located as close to the nozzle throat as is practical.

Lewis Flight Propulsion Laboratory
National Advisory Committee for Aeronautics
Cleveland, Ohio, April 26, 1955

APPENDIX A

SYMBOLS

The following symbols are used in this report:

A	area, sq ft
a	sonic velocity, ft/sec
D	time delay, sec
K	constant
L	length of respective component, ft
M	Mach number
$\frac{\Delta p}{q}$	pressure-drop coefficient associated with a flameholder
R	universal gas constant, 1716 $(ft/sec^2)(ft\text{-}lb/(lb)(^\circ R))$
r	radius
T	total temperature, $^\circ R$
u	local velocity, ft/sec
x	distance along a component
γ	ratio of specific heats
μ	1 + fuel-air ratio
τ	engine total-temperature ratio

Subscripts:

d	diffuser
e	exponential temperature distribution
f	fuel propagation
i	fuel-injection or diffuser-exit station

l	linear temperature distribution
n	nozzle
s	diffuser sensing station
w	wave propagation
x	distance along a component
0	free stream
1	engine inlet
2	fuel-injection-section exit
3	combustor inlet
4	combustor exit
5	nozzle throat
*	position where $M = 1$

APPENDIX B

DERIVATION OF EQUATIONS FOR COMPONENT TIME DELAYS

Equations are derived herein for the time delays of the several engine components discussed in the body of the report. The results of these equations are plotted in figures 4 to 11.

Consider a duct through which a compressible fluid is flowing, such as the engine component 1 to 2 of the following sketch:

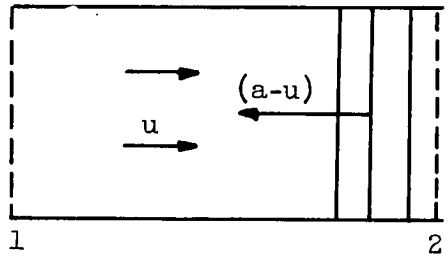

Sketch (a)

Fluid particles in the stream travel downstream from 1 to 2 at the local air velocity u. The time required for this particle travel is termed fluid-propagation time, which can be expressed mathematically as

$$D_f = \int_1^2 \frac{dx}{u} = \int_1^2 \frac{1}{\sqrt{\gamma RT}} \frac{\sqrt{1 + \frac{\gamma - 1}{2} M^2}}{M} dx \qquad (1)$$

If for some reason a disturbance occurs at station 2, the pressure wave generated by this disturbance travels upstream at the local speed of sound minus the local downstream air velocity a - u. The time consumed for this wave travel is termed wave-propagation time. Expressed mathematically,

$$D_w = \int_2^1 \frac{dx}{(a - u)} = \int_2^1 \frac{1}{\sqrt{\gamma RT}} \frac{\sqrt{1 + \frac{\gamma - 1}{2} M^2}}{(1 - M)} dx \qquad (2)$$

The total time delay D in the response of a ram-jet engine to an imposed fuel-flow step is assumed to be the fluid-propagation time from the fuel injector to the exhaust-nozzle throat plus the wave-propagation time from the exhaust-nozzle throat to the point at which the response is measured. Hence, from equations (1) and (2),

$$D = D_f + D_w = \frac{1}{\sqrt{\gamma R}} \int_1^2 \frac{(1 - 2M)}{M(1 - M)} \sqrt{1 + \frac{\gamma - 1}{2} M^2} \frac{dx}{\sqrt{T}} \qquad (3)$$

This problem is resolved by expressing $dx/\sqrt{T}$ in terms of Mach number for the following three general cases: (1) where total temperature and Mach number remain constant throughout the component (fuel-injection section and diffuser straight section); (2) where total temperature remains constant but Mach number changes (nozzle and diffuser); and (3) where both total temperature and Mach number change (combustion chamber).

Fuel-Injection Section and Diffuser Straight Section

In the fuel-injection section, the fuel was assumed to travel at the local downstream air velocity (ref. 4) in a constant-area pipe (Sketch (a)). Therefore, the fluid-propagation time per unit length is simply $1/u$. Also, a pressure wave moving upstream travels at the local speed of sound minus the local downstream velocity $a - u$. Therefore, the wave-propagation time per unit length is $1/(a - u)$. The resulting time delay $\frac{1}{u} + \frac{1}{a - u}$ is plotted in figure 4.

Constant-area sections may also be placed in a diffuser. The wave-propagation time per unit length in this section is simply $1/(a - u)$, which is plotted in figure 11.

Nozzle and Diffuser

The exhaust nozzle and diffuser are similar in that an area variation produces the desired change in Mach number. Both sections were assumed to have constant ratio of specific heats γ, total temperature T, and linear variation in radius with length. However, in the nozzle γ equaled 1.3 and the temperature equaled T_4, while in the diffuser γ equaled 1.4 and the temperature equaled T_1. In these sections, the one-dimensional area-variation equation is used to transform the variable to Mach number. Since the nozzle was choked,

$$\frac{A_*}{A} = M\left(\frac{\frac{\gamma + 1}{2}}{1 + \frac{\gamma - 1}{2} M^2}\right)^{\frac{\gamma+1}{2(\gamma-1)}} \qquad (4)$$

The radius of the nozzle may be expressed mathematically as

$$r = \left(\frac{\sqrt{A_*} - \sqrt{A_4}}{L\sqrt{\pi}}\right)x + \sqrt{\frac{A_4}{\pi}} \tag{5}$$

Equation (5) is substituted into equation (4); the result, upon differentiation, is inserted into equations (1) and (2). The integrand of D is then expanded by use of the binomial theorem and integrated. Since M_4 is less than unity, and because the coefficients of the higher powers approach zero, terms of higher degree than 5/2 may be neglected. The integration gives

$$\frac{D}{L} \cong K_n\left[-2.1 + 2\left(\frac{1}{M_4^{1/2}} + \frac{1}{3M_4^{3/2}} - 0.212\,M_4^{1/2} - 0.071\,M_4^{3/2}\right)\right] \tag{6}$$

where $$K_n = \frac{1}{2\sqrt{\gamma RT}\left(\sqrt{\frac{A_4}{A_*}} - 1\right)\left(\frac{\gamma+1}{2}\right)^{\frac{\gamma+1}{4(\gamma-1)}}}$$

The solution of this equation, in terms of temperature and area ratios, is given in figure 9. Neglecting higher orders of Mach number in this expansion (6) is not critical, since the time delay of the nozzle is only approximately 10 percent of the total time delay.

In the diffuser, neither station s nor i is assumed choked; equation (4) therefore was transformed into

$$A = \frac{A_i M_i}{M}\left(\frac{1 + \frac{\gamma-1}{2}M^2}{1 + \frac{\gamma-1}{2}M_i^2}\right)^{\frac{\gamma+1}{2(\gamma-1)}} \tag{7}$$

The radius of the diffuser may be expressed mathematically as

$$r = \left(\frac{\sqrt{A_i} - \sqrt{A_s}}{L\sqrt{\pi}}\right)x + \sqrt{\frac{A_s}{\pi}} \tag{8}$$

Equation (8) is substituted into equation (7) which, upon differentiation, is inserted into equation (2). With the assumption of $\gamma = 1.4$, D_w integrates in closed form. Hence,

$$\frac{D_w}{L} = K_d\left[2\left(M_s^{1/2} - M_i^{1/2}\right) + \frac{\gamma - 1}{5}\left(M_s^{5/2} - M_i^{5/2}\right) - 2\left(\frac{1}{M_s^{1/2}} - \frac{1}{M_i^{1/2}}\right) + \frac{\gamma - 1}{3}\left(M_s^{3/2} - M_i^{3/2}\right)\right] \tag{9}$$

where $$K_d = \frac{1}{2\left(\frac{\gamma + 1}{2}\right)^{\frac{\gamma+1}{4(\gamma-1)}}\sqrt{\gamma RT}\left(\sqrt{\frac{A_s}{A_*}} - \sqrt{\frac{A_i}{A_*}}\right)}$$

Equation (9) is plotted in figure 10.

Combustion Chamber

For the combustor, a simplified steady-state one-dimensional heat-addition equation in a constant-area tube is used to transform the variable to Mach number:

$$\frac{M\left(1 + \frac{\gamma - 1}{2}M^2\right)^{1/2}}{1 + \gamma M^2} = \mu\sqrt{\frac{T}{T_3}}\frac{M_3\left(1 + \frac{\gamma - 1}{2}M_3^2\right)^{1/2}}{1 + \gamma M_3^2} \tag{10}$$

For simplicity, R and γ are assumed constant over the full length of the combustion chamber at 1716 $(ft/sec^2)(ft\text{-}lb/(lb)(^oR))$ and 1.3, respectively. Equation (10) solved for T is

$$T = \frac{M^2}{M_3^2}\frac{(1 + \gamma M_3^2)^2}{(1 + \gamma M^2)^2}\frac{\left(1 + \frac{\gamma - 1}{2}M^2\right)}{\left(1 + \frac{\gamma - 1}{2}M_3^2\right)}\frac{T_3}{\mu^2} \tag{11}$$

However,

$$T = f(x) \tag{12}$$

which varies, depending upon the rate of heat addition assumed. Equations (11) and (12) are combined and differentiated with respect to x and M. When the result is substituted into equations (1) and (2), the transformation of variable is complete.

Linear distribution of T. - Substitution of the proper boundary conditions into the equation of a straight line results in the following equation:

$$T = (T_4 - T_3)\frac{x}{L} + T_3 \tag{13}$$

Upon substitution of equation (13) into equations (12) and (11) and integration, the resulting equation is

$$\frac{D}{L} = K_l\left\{\frac{1}{2}\ln\frac{M_4^2}{M_3^2}\left(\frac{1+\gamma M_3^2}{1+\gamma M_4^2}\right) + \frac{M_4+1}{2(1+\gamma M_4^2)} - \frac{M_3+1}{2(1+\gamma M_3^2)} + \frac{1}{2\sqrt{\gamma}}\left[\tan^{-1}(M_4\sqrt{\gamma}) - \tan^{-1}(M_3\sqrt{\gamma})\right]\right\} \tag{14}$$

where $K_l = \dfrac{2(1+\gamma M_3^2)}{(T_4 - T_3)\mu\sqrt{\dfrac{\gamma R\left(1+\frac{\gamma-1}{2}M_3^2\right)}{T_3}}}$

A solution of equation (14) converted to τ and u_3 is plotted in figure 7.

Sinusoidal distribution of T. - The equation for the first 90° of a sine curve, with the proper boundary conditions, is

$$T = (T_4 - T_3)\sin\frac{\pi}{2}\frac{x}{L} + T_4 \tag{15}$$

Upon substitution of equation (15) into equations (12) and (11), an improper integral is obtained, which is unintegrable in closed form. A suitable approximation can be made to the sine variation by employing a number of straight-line segments representing linear variations in T. As is apparent, the accuracy of the approximation improves with the number of segments. A three-segment approximation (fig. 3) was used for the results of figure 6.

Exponential distribution of T. - The equation of an exponential distribution, with the proper boundary conditions, is

$$T = \left(\frac{T_4 - T_3}{e-1}\right)e^{x/L} + \left(\frac{eT_3 - T_4}{e-1}\right) \tag{16}$$

Substitution of equation (16) into equations (12) and (11) yields

$$\frac{D}{L} = K_e \int_{M_3}^{M_4} \frac{(1 + M)dM}{M\left\{M^2\left(1 + \frac{\gamma-1}{2} M^2\right) - \left(\frac{eT_3 - T_4}{e - 1}\right)\left[\frac{\mu^2}{T_3}\frac{\left(1 + \frac{\gamma-1}{2} M_3^2\right)}{(1 + \gamma M_3^2)}\right](1 + \gamma M^2)^2\right\}} \tag{17}$$

where $K_e = \frac{2\mu}{(1 + \gamma M_3^2)}\sqrt{\frac{1 + \frac{\gamma - 1}{2} M_3^2}{\gamma R T_3}}$

A numerical integration is required, and the results, converted to τ and u_3, are given in figure 8.

Step-function distribution of T. - The calculations for the step-function distribution of temperature are similar to those for the fuel-mixing section because of the constant area and total temperature in the combustor. Thus, the sum of fluid-propagation and wave-propagation time per unit length is simply $(1/u) + [1/(a - u)]$. This is plotted in figure 5.

REFERENCES

1. Vasu, G., Wilcox, F. A., and Himmel, S. C.: Preliminary Report of a Experimental Investigation of Ram-Jet Controls and Engine Dynamics. NACA RM E54H10, 1954.

2. Wilcox, Fred A., Perchonok, Eugene, and Hearth, Donald P.: Investigation of an On-Off Inlet Shock-Position Control on a 16-Inch Ram-Jet Engine. NACA RM E54I21, 1954.

3. Dunbar, William R., Vasu, George, and Hurrell, H. George: Experimental Investigation of Direct Control of Diffuser Pressure on 16-Inch Ram-Jet Engine. NACA RM E55D15, 1955.

4. Ingebo, Robert D.: Vaporization Rates and Drag Coefficients for Isooctane Sprays in Turbulent Air Streams. NACA TN 3265, 1954.

5. Koffel, William K., and Kaufman, Harold R.: Empirical Cooling Correlation for an Experimental Afterburner with an Annular Cooling Passage. NACA RM E52C13, 1952.

6. Donlon, Richard H., McCafferty, Richard J., and Straight, David M.: Investigation of Transient Combustion Characteristics in a Single Tubular Combustor. NACA RM E53L10, 1954.

7. Hearth, Donald P., and Perchonok, Eugene: Performance of a 16-Inch Ram-Jet Engine with a Can-Type Combustor at Mach Numbers of 1.50 to 2.16. NACA RM E54G13, 1954.

TABLE I. - EFFECT OF ASSUMED TEMPERATURE DISTRIBUTION ON COMBUSTOR TIME DELAY

[Conditions at fuel-injection-section exit: Mach number, 0.20; temperature, 705° R. Total-temperature ratio, 4.]

Type of distribution	Time delay, sec/ft
Step function	0.00163
Sine	.00228
Linear	.00256
Exponential	.00286

TABLE II. - EFFECT OF FLAMEHOLDER ON COMBUSTOR TIME DELAY

[Sine temperature variation; free-stream Mach number, 2.0; total-temperature ratio, 4; flameholder pressure-drop coefficient, 2.3.]

Without flameholder		With flameholder		Difference, $\frac{\Delta D_{2-3}}{D_3}$, percent
Mach number, M_2	Time delay, D_2, sec/ft	Mach number, M_3	Time delay, D_3, sec/ft	
0.10	0.00374	0.102	0.00369	1.34
.15	.00275	.156	.00268	2.54
.20	.00228	.213	.00224	1.75
.215	.00223	.232	.00260	-16.60

TABLE III. - COMPONENT TIME DELAY OF 16-INCH RAM-JET ENGINE

[Conditions at fuel-injection-section exit: Mach number, 0.185; temperature, 590° R. Combustor-exit Mach number, 0.459; total-temperature ratio, 4]

Engine component	Time delay, sec	Percent of total time
Fuel-mixing section	0.0060	22.2
Combustion chamber	.0143	52.8
Exhaust nozzle	.0033	12.1
Diffuser (station s to i, fig. 12)	.0035	12.9
Total	0.0271	100.0

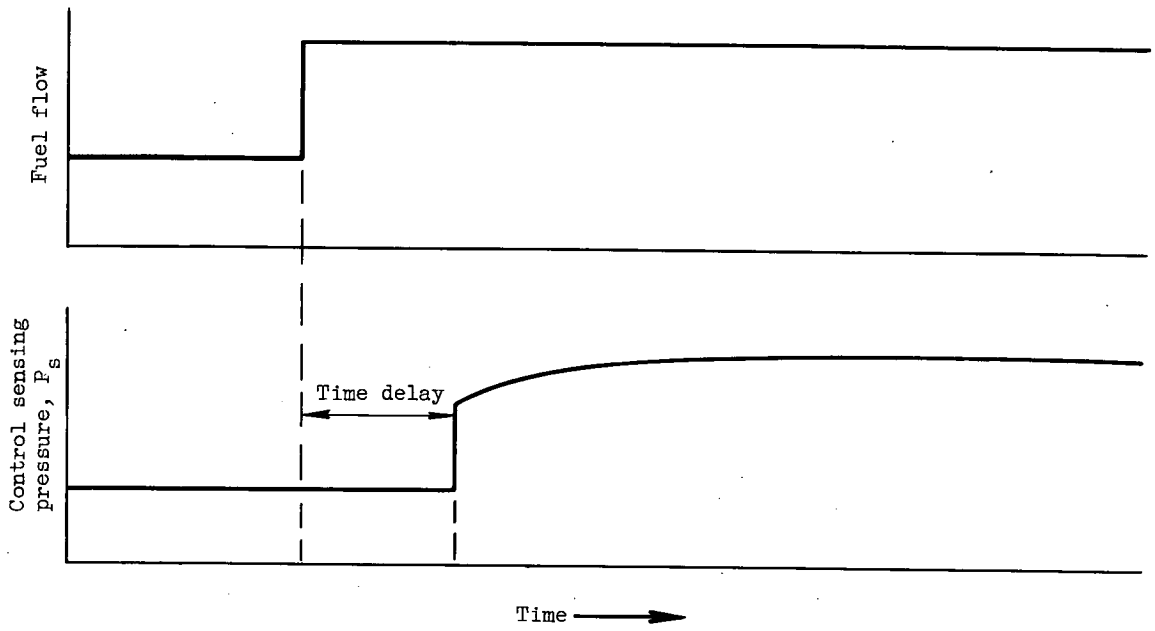

Figure 1. - Engine response to step change in fuel flow.

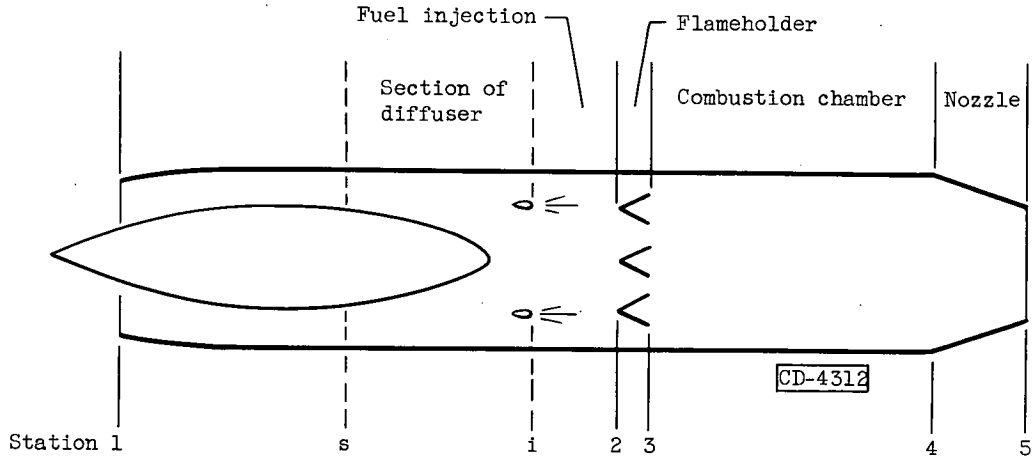

Figure 2. - Schematic diagram of ram-jet engine.

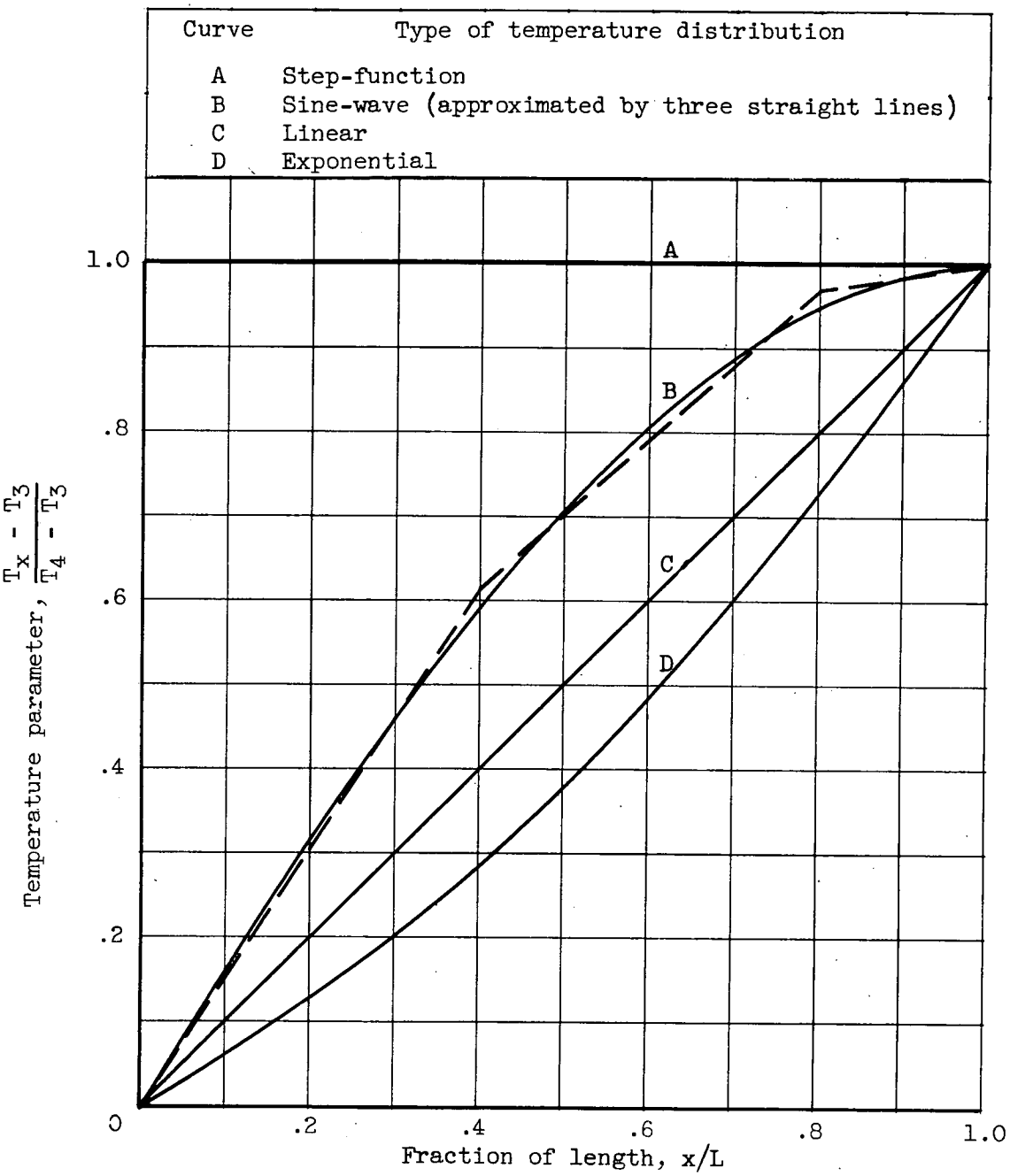

Figure 3. - Temperature-distribution curves used in combustion-chamber analysis.

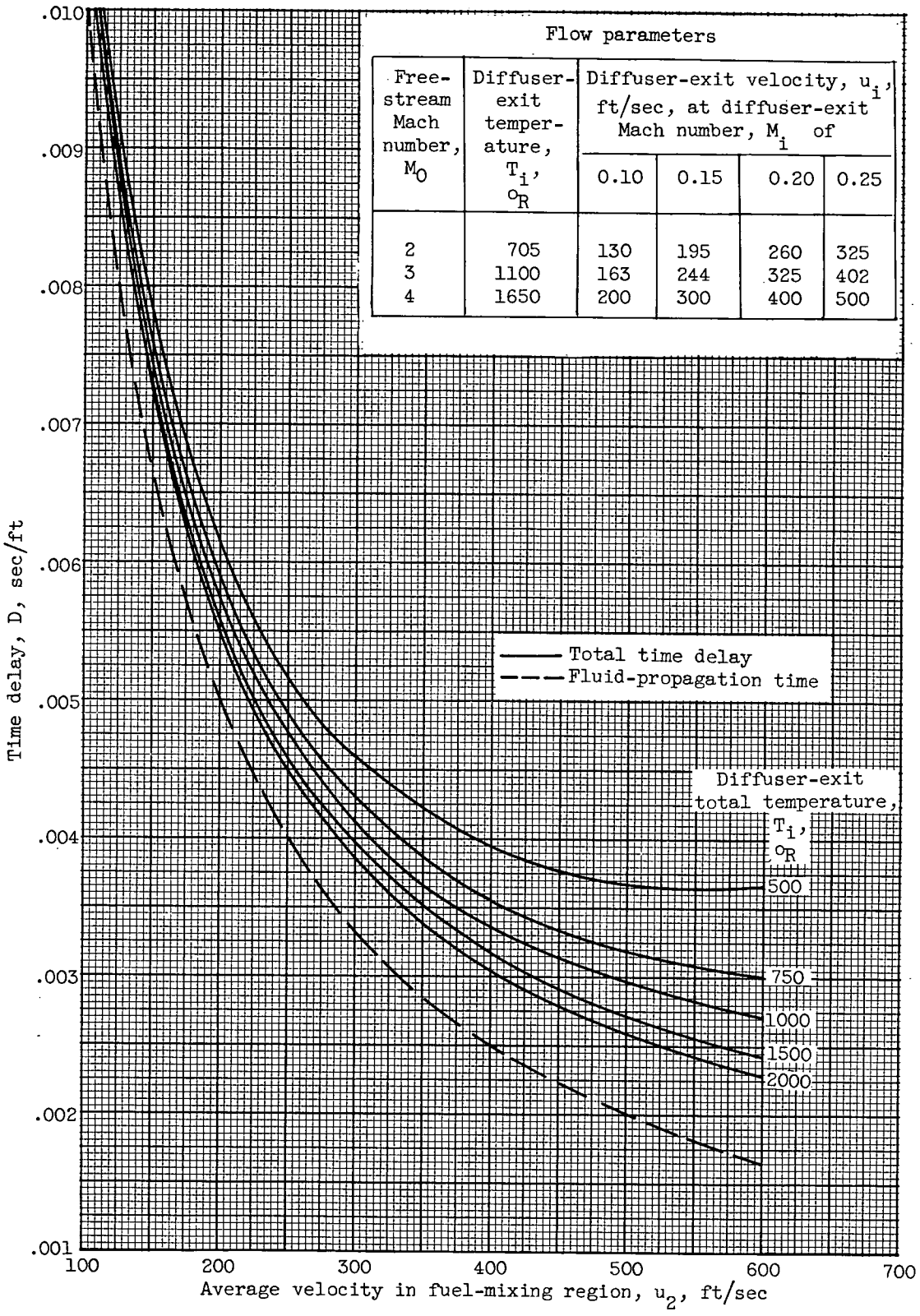

Figure 4. - Time delay in a constant-area fuel-mixing region.

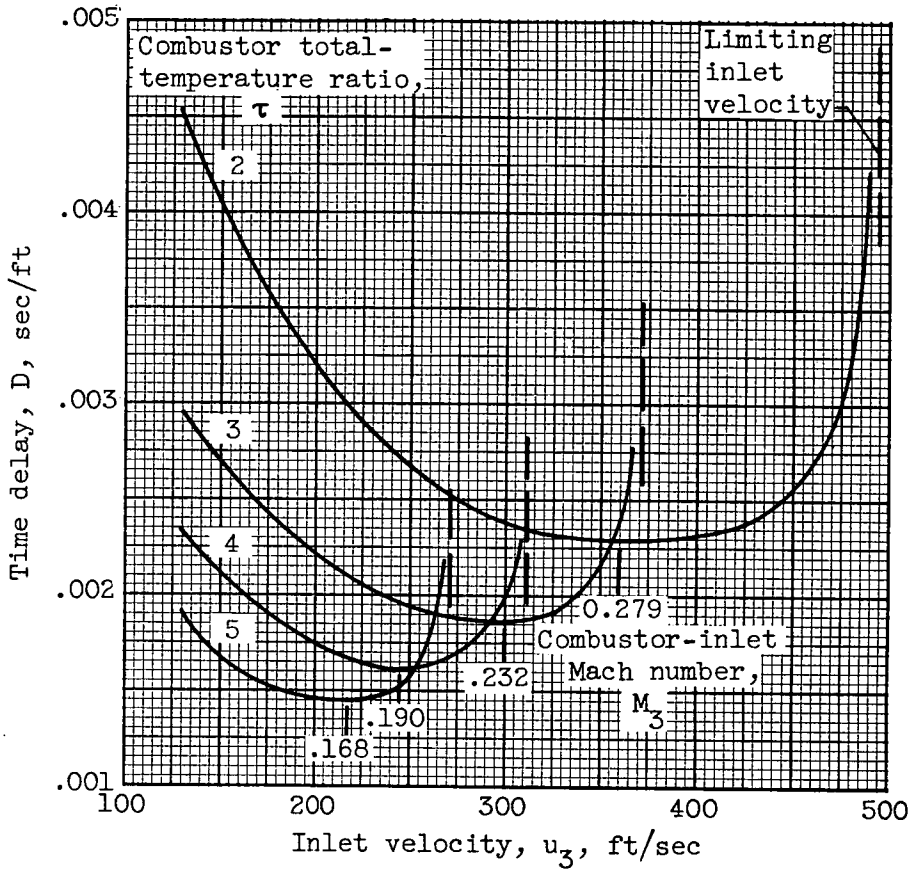

(a) Free-stream Mach number, 2.0.

Figure 5. - Combustor time delay for step-function temperature distribution.

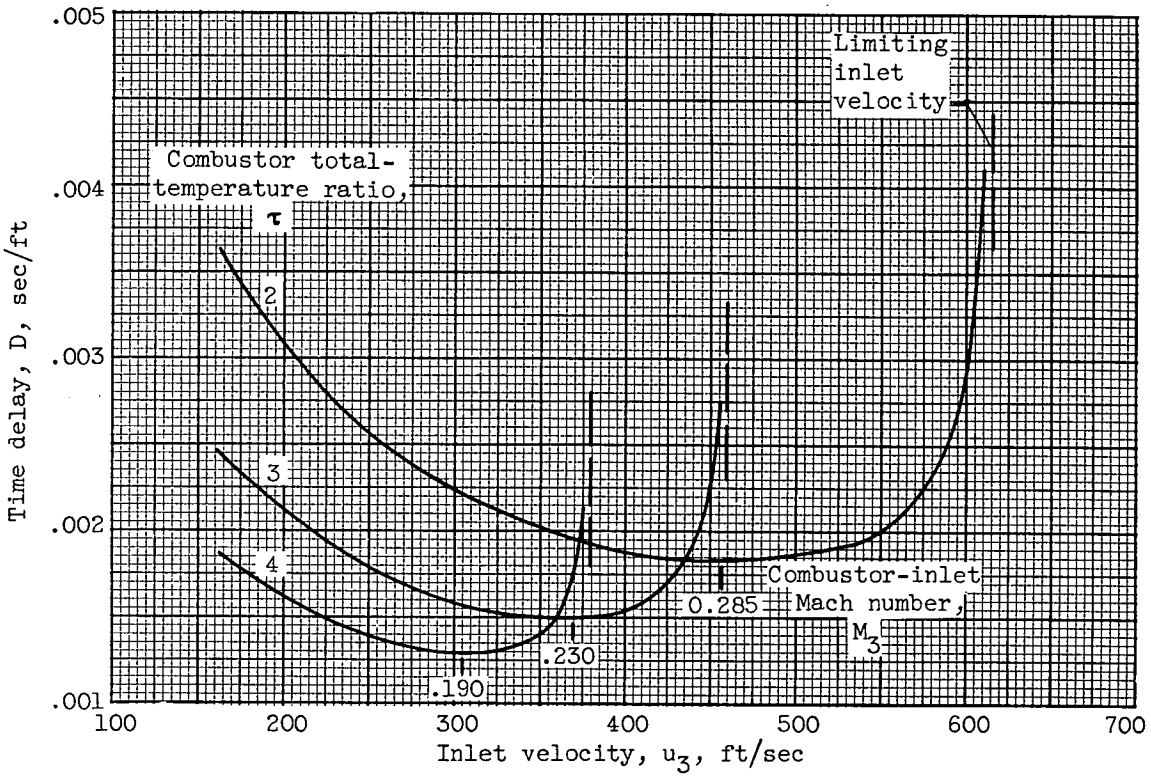

(b) Free-stream Mach number, 3.0.

Figure 5. - Continued. Combustor time delay for step-function temperature distribution.

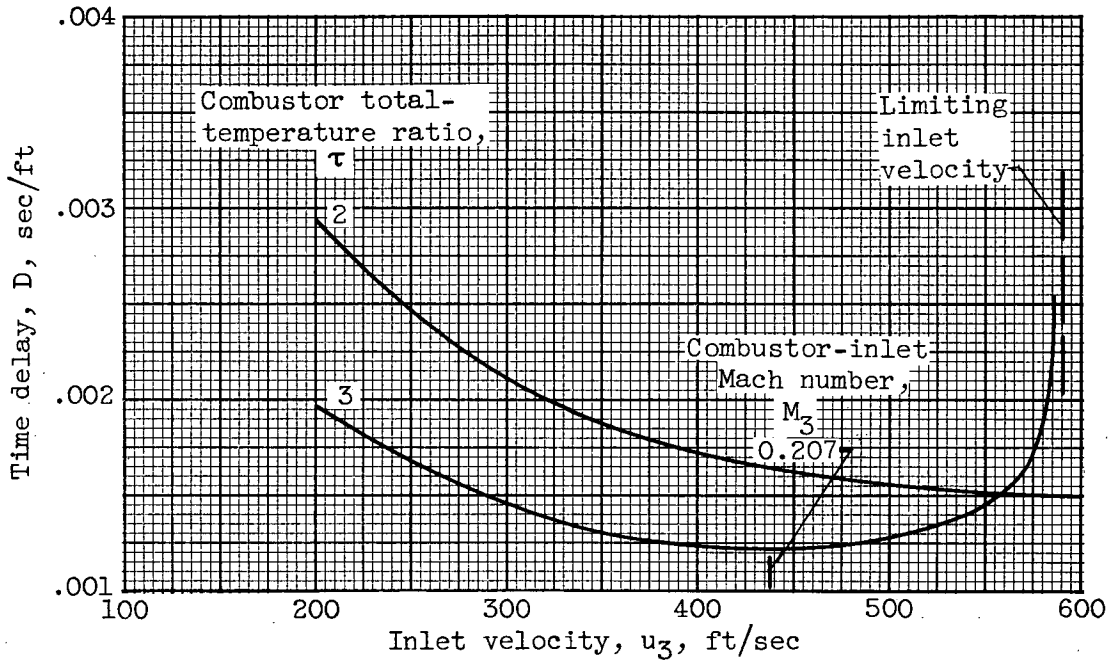

(c) Free-stream Mach number, 4.0.

Figure 5. - Concluded. Combustor time delay for step-function temperature distribution.

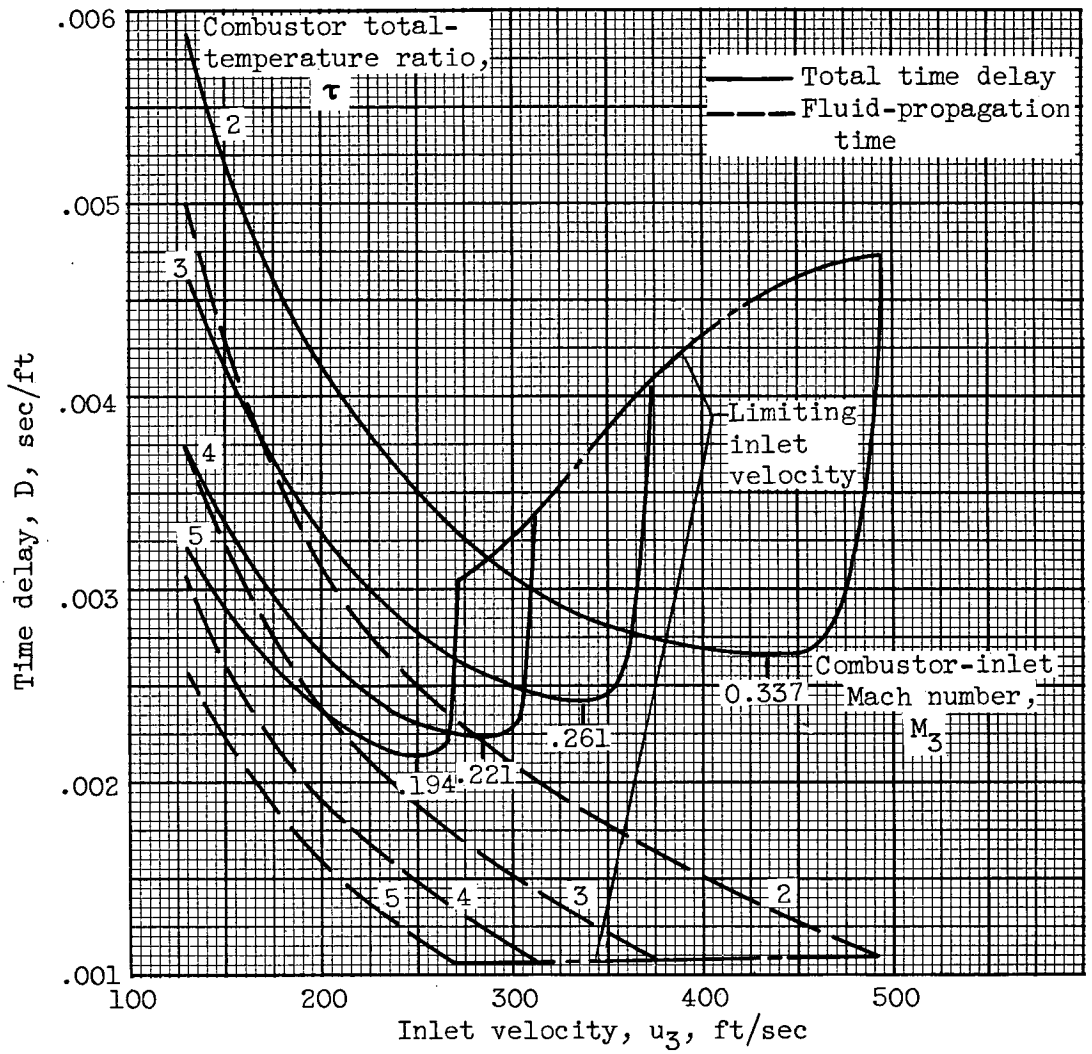

(a) Free-stream Mach number, 2.0.

Figure 6. - Combustor time delay for sinusoidal temperature distribution.

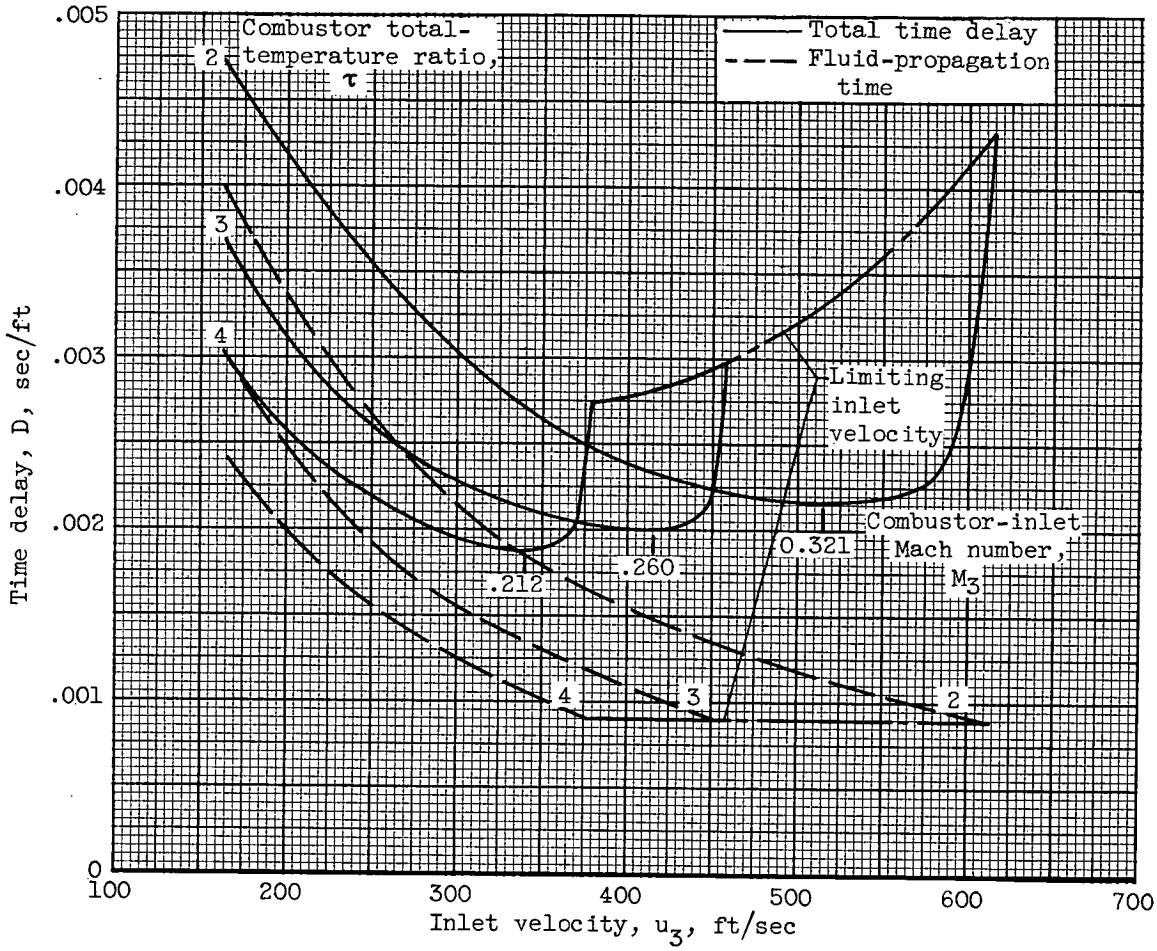

(b) Free-stream Mach number, 3.0.

Figure 6. - Continued. Combustor time delay for sinusoidal temperature distribution.

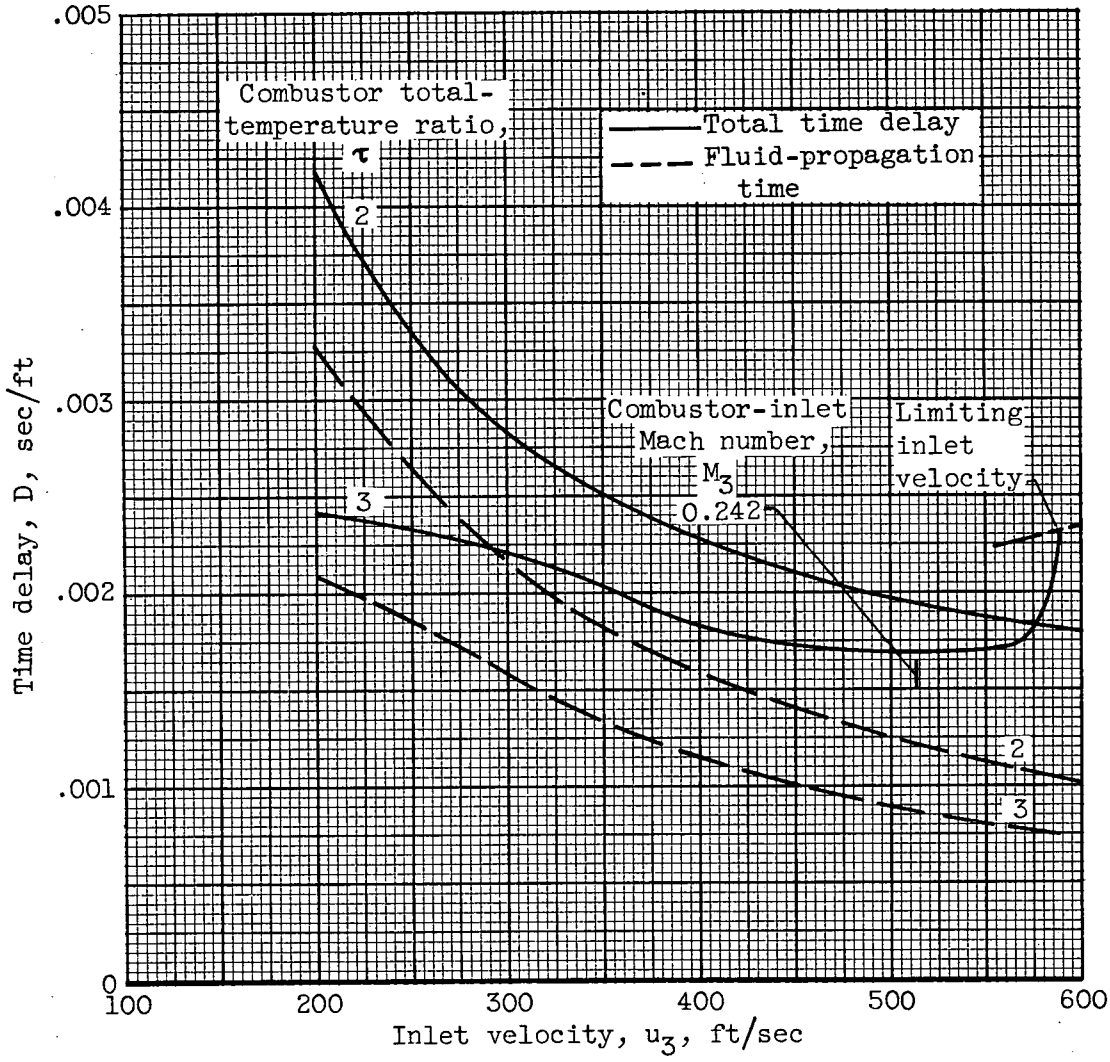

(c) Free-stream Mach number, 4.0.

Figure 6. - Concluded. Combustor time delay for sinusoidal temperature distribution.

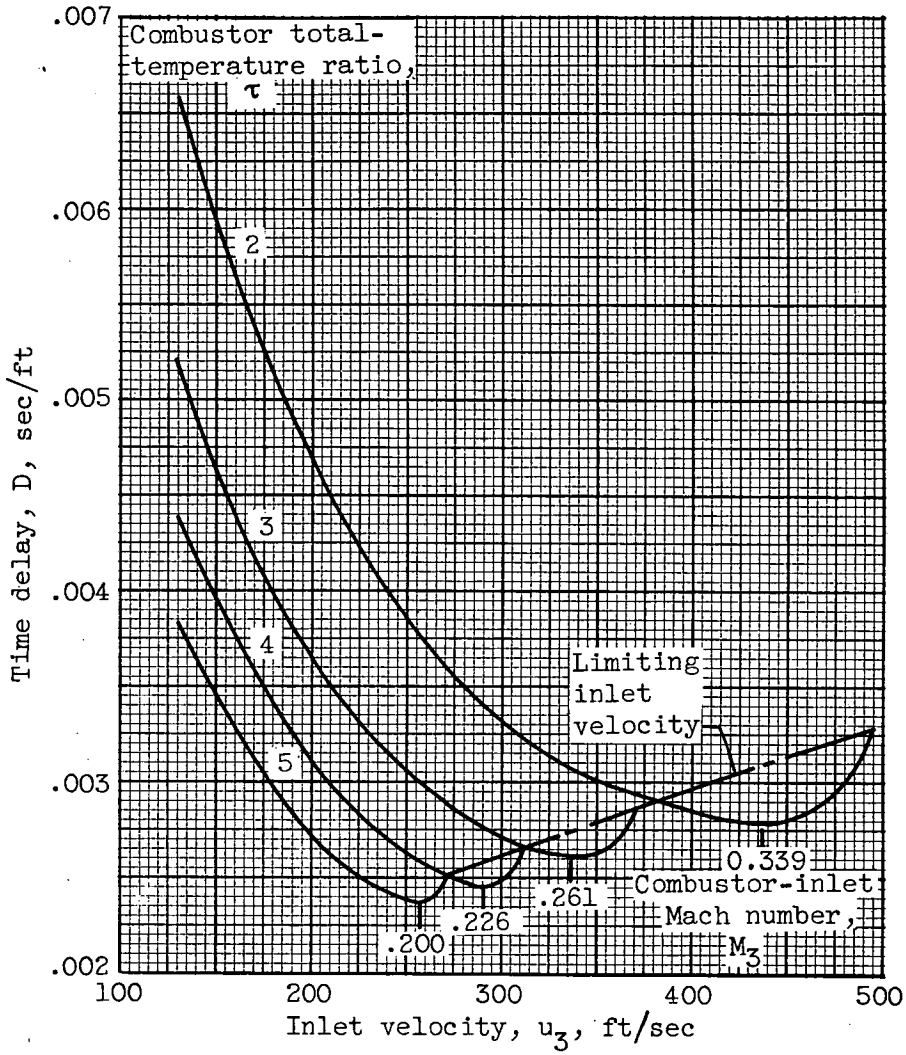

(a) Free-stream Mach number, 2.0.

Figure 7. - Combustor time delay for linear temperature distribution.

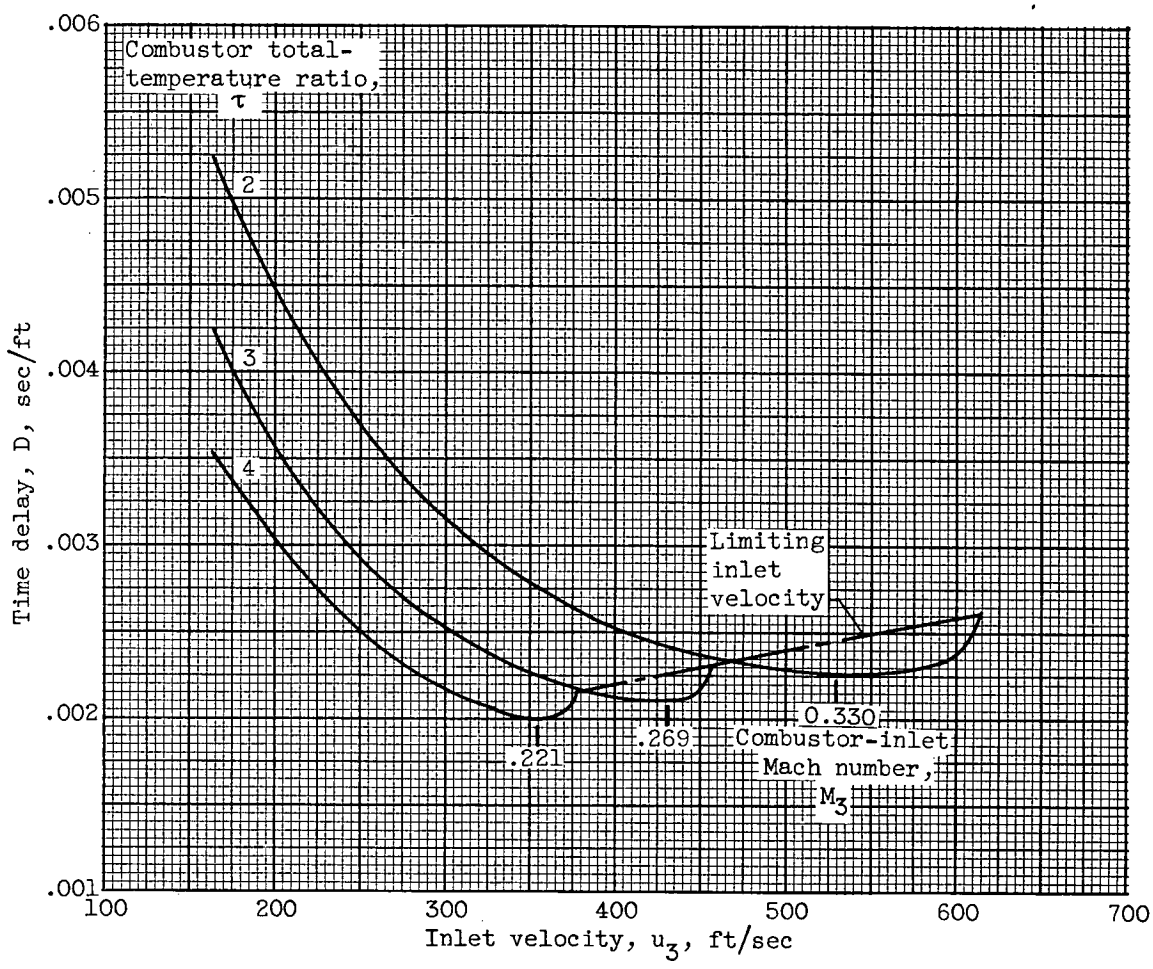

(b) Free-stream Mach number, 3.0.

Figure 7. - Continued. Combustor time delay for linear temperature distribution.

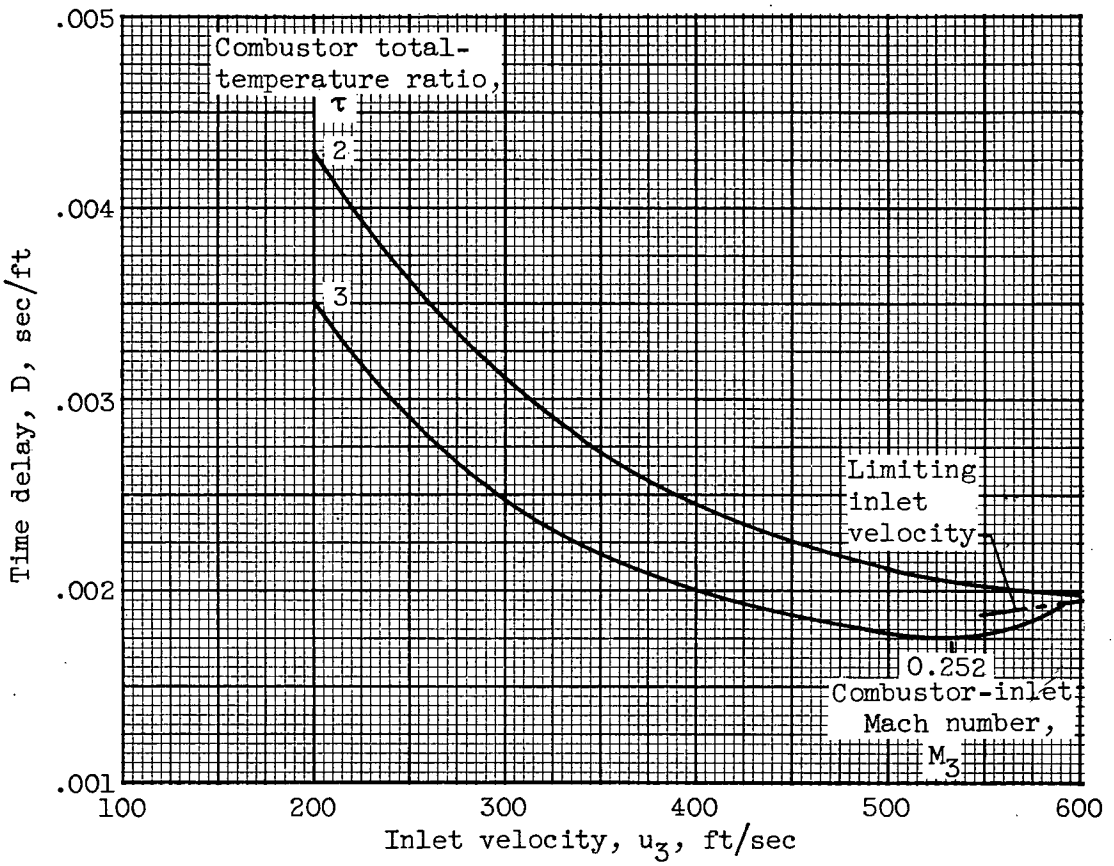

(c) Free-stream Mach number, 4.0.

Figure 7. - Concluded. Combustor time delay for linear temperature distribution.

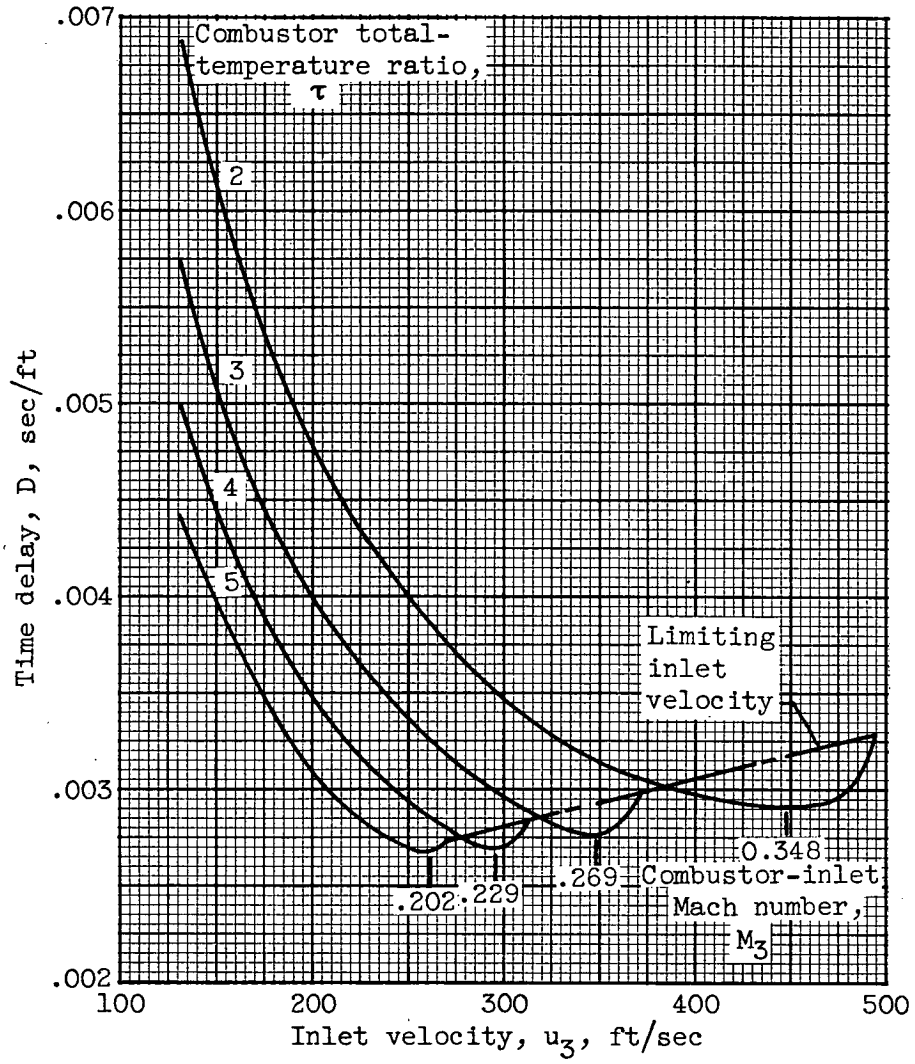

(a) Free-stream Mach number, 2.0.

Figure 8. - Combustor time delay for exponential temperature distribution.

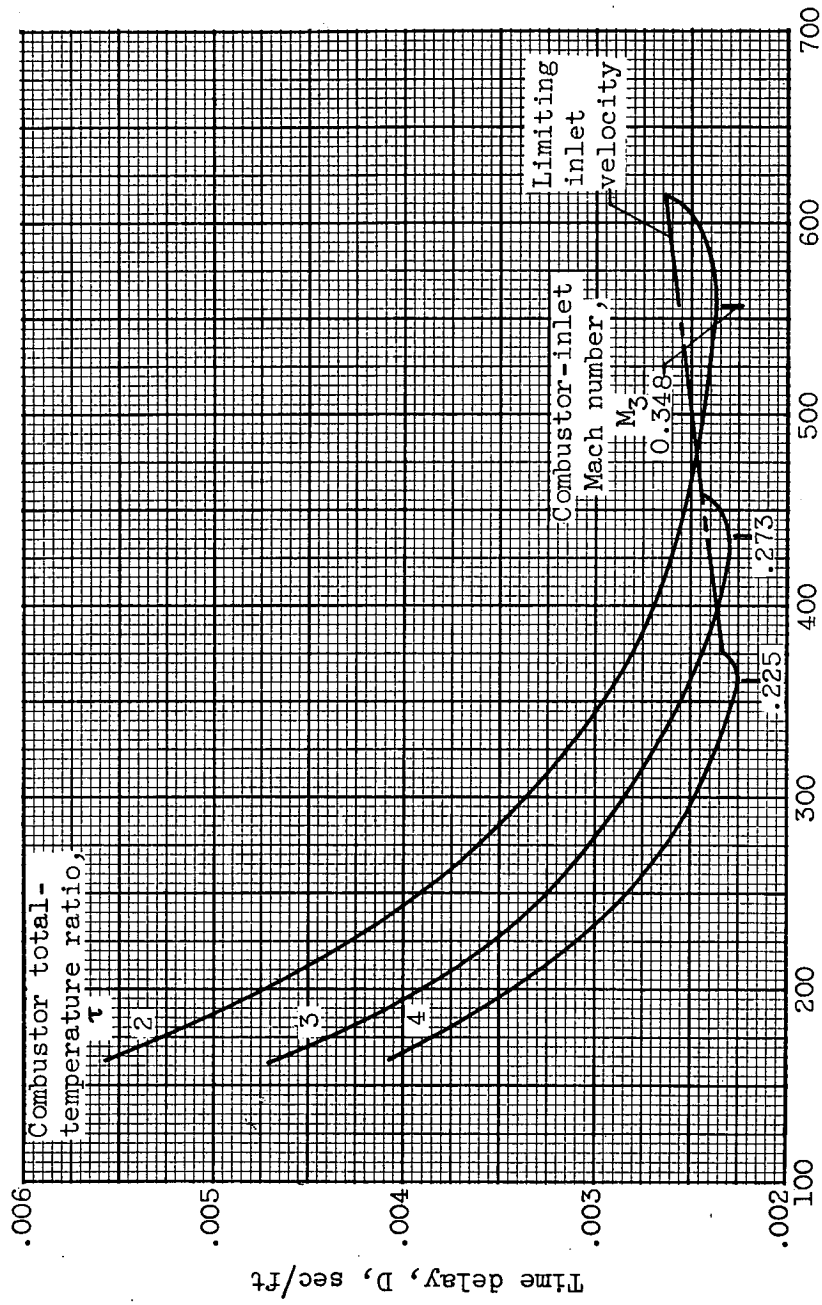

(b) Free-stream Mach number, 3.0.

Figure 8. - Continued. Combustor time delay for exponential temperature distribution.

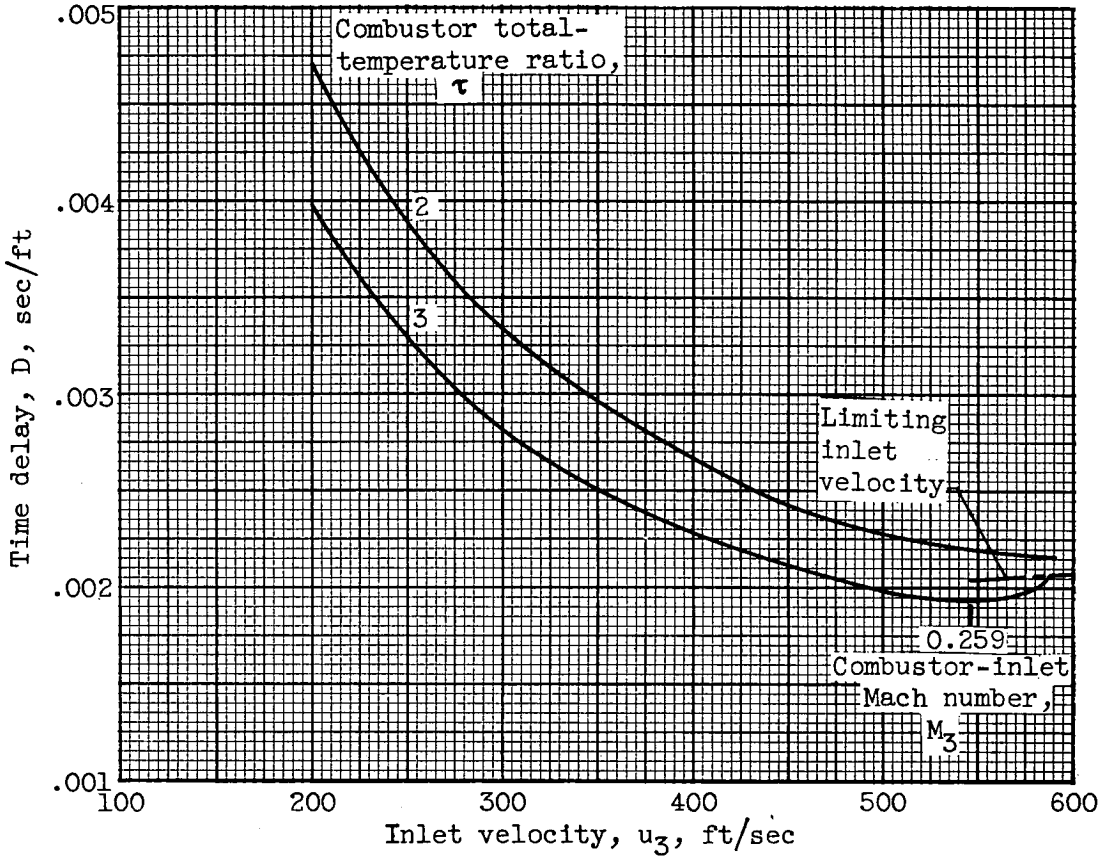

(c) Free-stream Mach number, 4.0.

Figure 8. - Concluded. Combustor time delay for exponential temperature distribution.

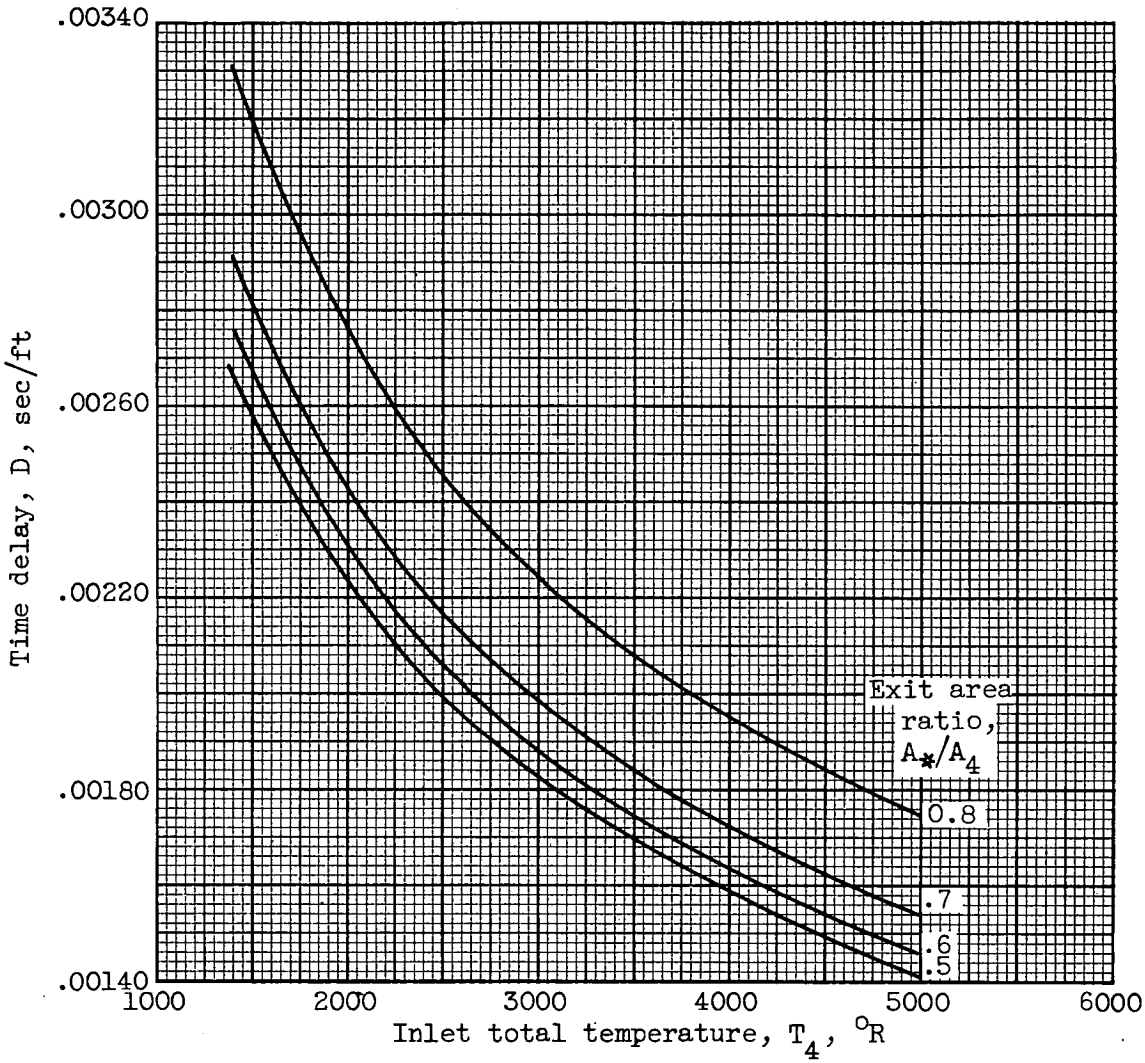

Figure 9. - Time delay in conical exhaust nozzle.

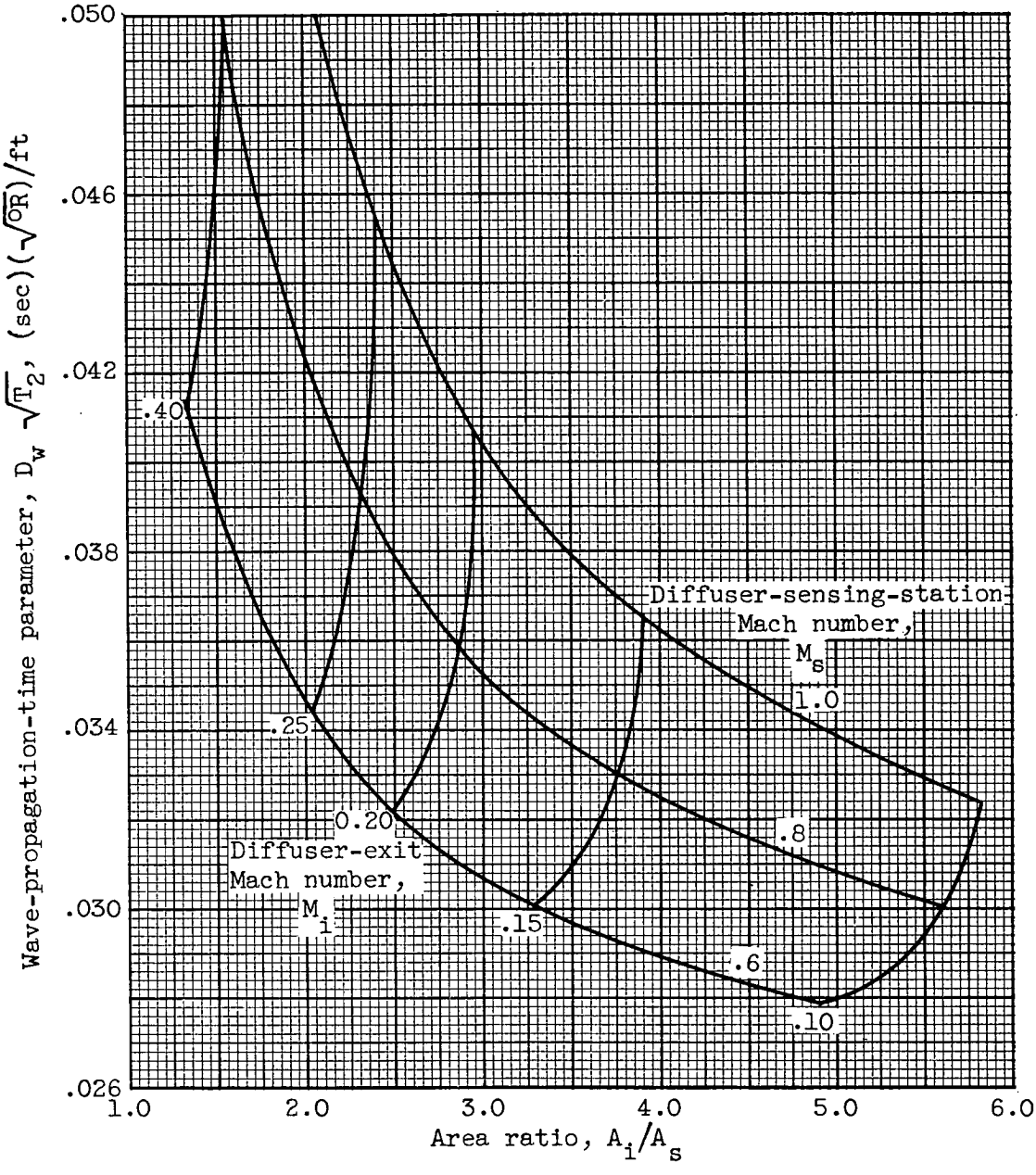

Figure 10. - Wave-propagation-time parameter for subsonic diffuser.

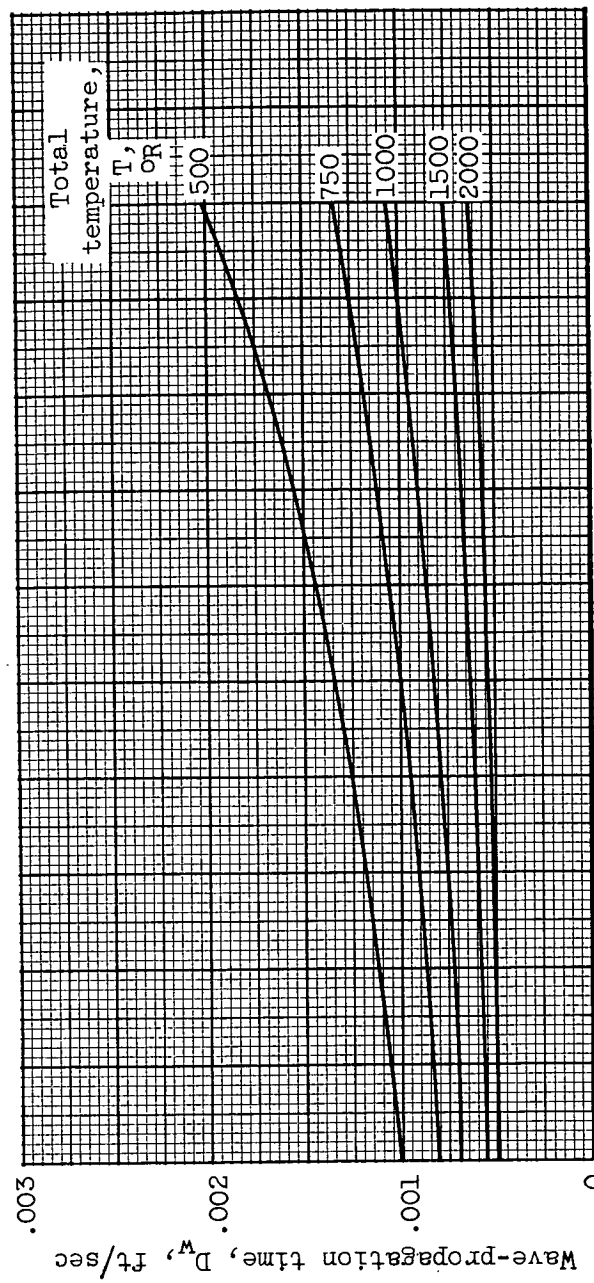

Figure 11. - Wave-propagation time through constant-area section.

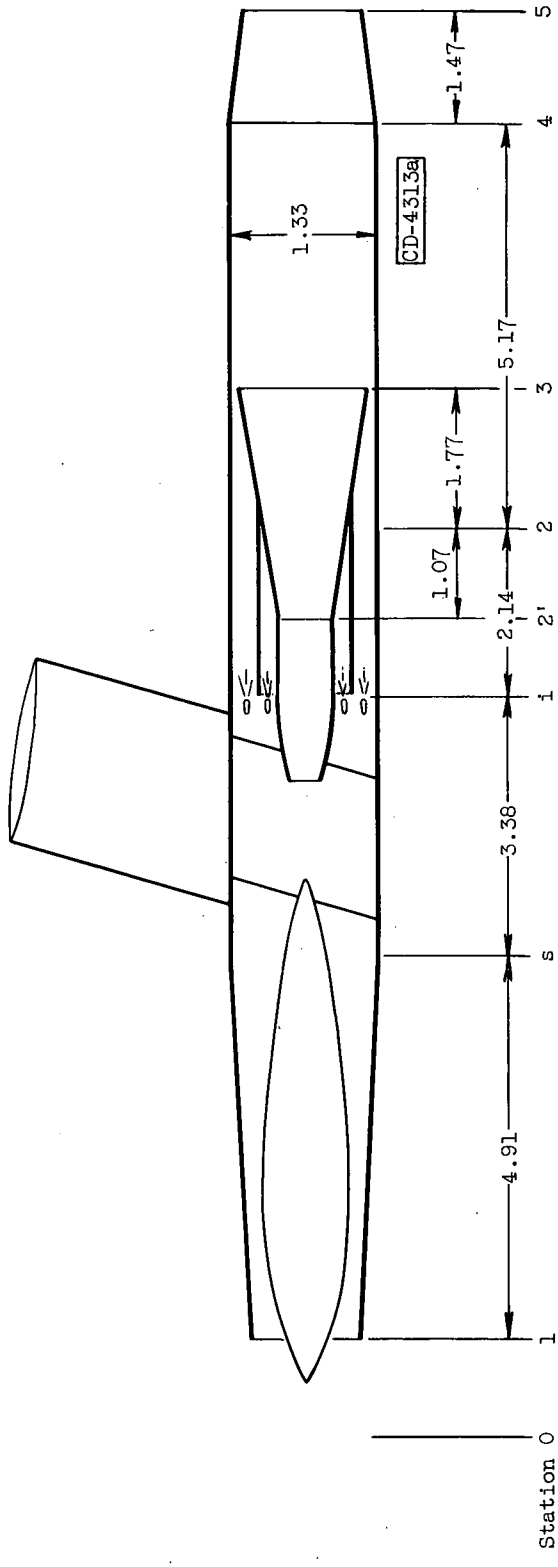

Figure 12. - Schematic diagram of 16-inch ram-jet engine (axially symmetric inlet). Area ratio, A_5/A_4, 0.7. (All dimensions in feet.)

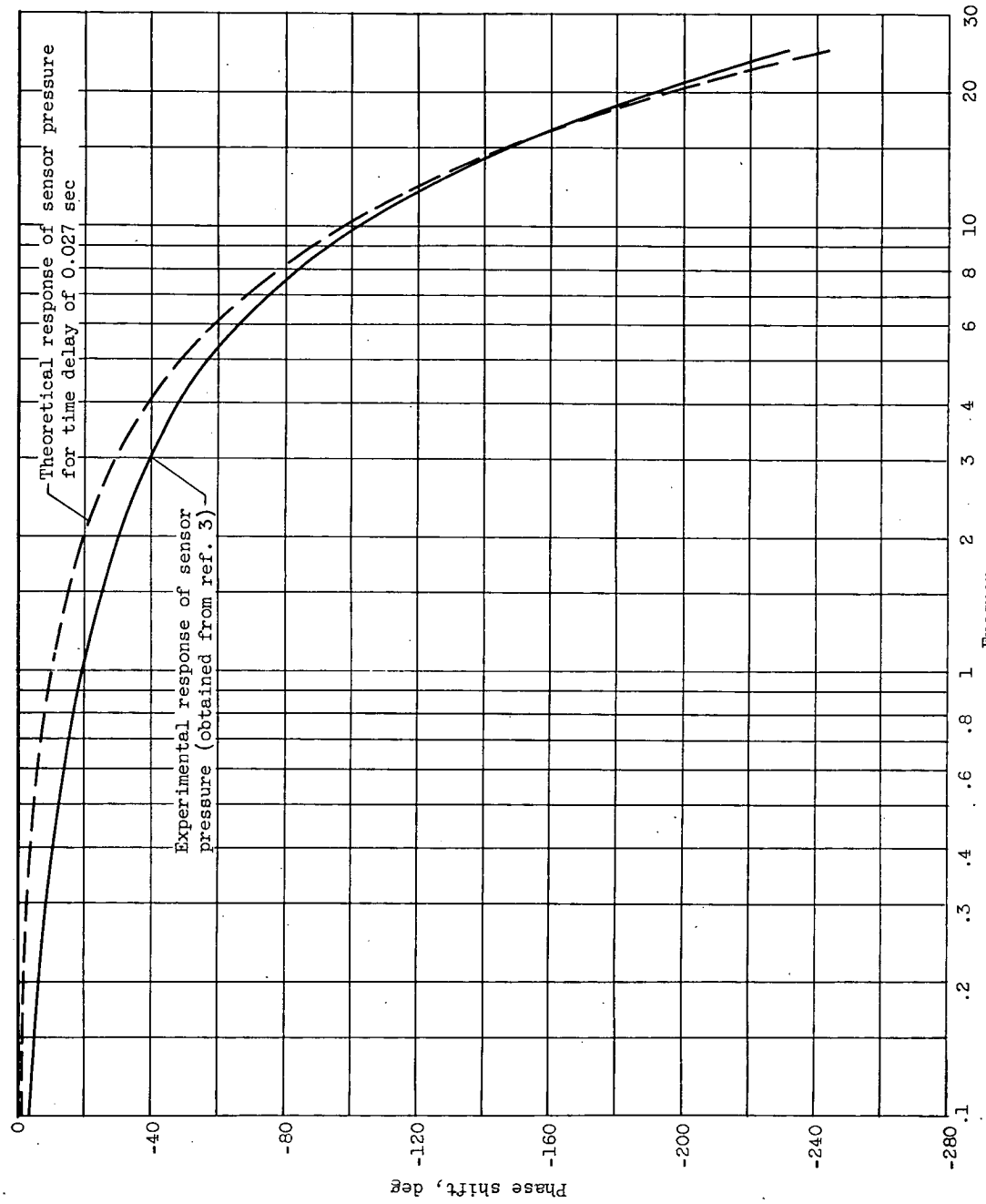

Figure 13. - Experimental and theoretical phase-shift-frequency characteristics of 16-inch ram-jet engine.

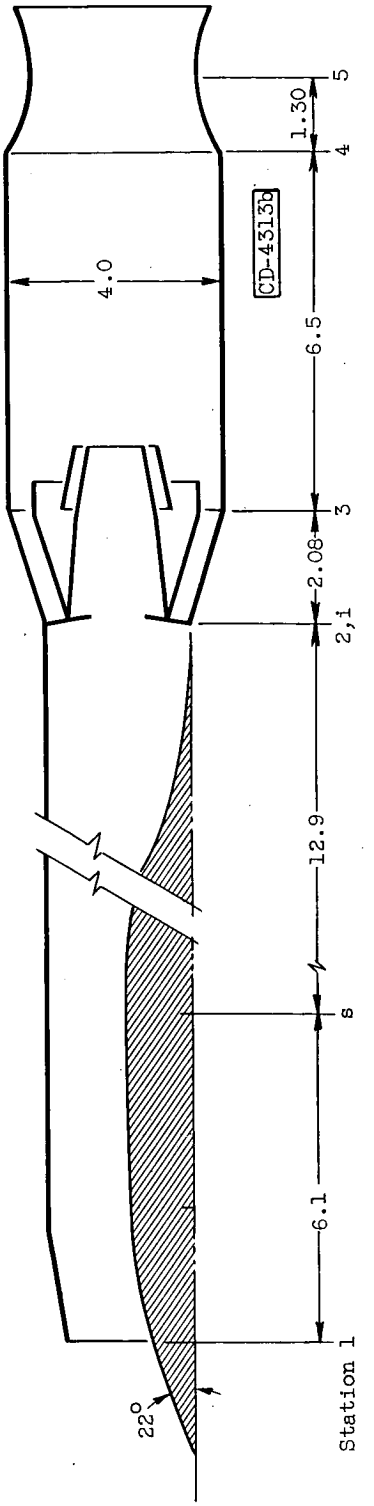

Figure 14. - Schematic diagram of 48-inch submerged ram-jet engine (side inlet). Area ratio, A_5/A_4, 0.56. (All dimensions in feet.)

NACA-Langley - 6-30-55 - 350